Bioconjugate Chemistry

ARTICLE

pubs.acs.org/bc

DNA Gold Nanoparticle Conjugates Incorporating Thiooxonucleosides: 7-Deaza-6-thio-2′-deoxyguanosine as Gold Surface Anchor

Frank Seela,*[,†,‡] Ping Ding,[†,‡] and Simone Budow[†]

[†]Laboratory of Bioorganic Chemistry and Chemical Biology, Center for Nanotechnology, Heisenbergstrasse 11, 48149 Münster, Germany

[‡]Laboratorium für Organische und Bioorganische Chemie, Institut für Chemie, Universität Osnabrück, Barbarastrasse 7, 49069 Osnabrück, Germany

Supporting Information

ABSTRACT: A new protocol for the covalent attachment of oligonucleotides to gold nanoparticles was developed. Base-modified nucleosides with thiooxo groups were acting as molecular surface anchor. Compared to already existing conjugation protocols, the new linker strategy simplifies the synthesis of DNA gold nanoparticle conjugates. The phosphoramidite of 7-deaza-6-thio-2′-deoxyguanosine (**6**) was used in solid-phase synthesis. Incorporation of the sulfur-containing nucleosides can be performed at any position of an oligonucleotide; even multiple incorporations are feasible, which will increase the binding stability of the corresponding oligonucleotides to the gold nanoparticles. Oligonucleotide strands immobilized at the end of a chain were easily accessible during hybridization leading to DNA gold nanoparticle network formation. On the contrary, oligonucleotides immobilized *via* a central position could not form a DNA-AuNP network. Melting studies of the DNA gold nanoparticle assemblies revealed sharp melting profiles with a very narrow melting transition.

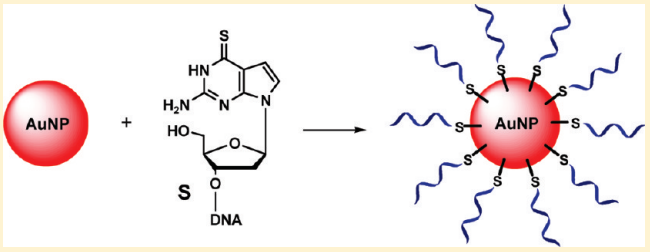

INTRODUCTION

DNA guided assemblies of metal nanoparticles have great potential for advanced material applications, in biomedical sciences, and as diagnostics tools.[1,2] DNA nanoparticle conjugates have been employed in nucleic acid detection and labeling and were utilized as barcodes, biosensors, or carriers for the delivery of DNA.[1−6] Additionally, they can be used for the bottom-up assembly of nanoarchitectures.[7,8] Among the accessible metal nanoparticles, gold nanoparticles (AuNPs) gained particular attention due to their chemical inertness and the ease of surface modification.[1,9,10] DNA gold nanoparticle (DNA-AuNP) conjugates combine the favorable properties of gold colloids with those of DNA. A number of key advantages for using the DNA molecule as a "construction material" are (i) its unique molecular recognition properties, (ii) its easy access by automated DNA synthesis or enzymatic polymerization, and (iii) its self-assembly capacities to form multistranded aggregates allowing the construction of DNA-based nanoscaled devices.[7,11]

To meet the above-mentioned applications, the conjugates must be stable in aqueous buffer systems, even at elevated temperature. For this, several strategies were developed for preparing DNA-AuNP conjugates.[12−15] The common protocol employs oligonucleotides with 3′ or 5′-terminal thiol groups introduced by linker units. The covalent attachment to AuNPs proceeds *via* the thiol functionality thereby making use of its strong affinity to the noble metal gold. There is still a controversial discussion on the mechanism of immobilization. However, an X-ray structure of a thiol monolayer protected gold nanoparticle has been reported recently.[16] Further developments in the field of DNA-AuNPs include the incorporation of sulfur functionalities into the oligonucleotide chain as an alternative to the conventional alkylthiol linker.[17,18] Phosphorothioate-modified DNA was utilized for gold nanoparticle conjugation either by directly coupling the DNA backbone to AuNPs[19] or by using a short linker molecule connecting the DNA backbone and the AuNPs.[20]

It is worth mentioning that tRNAs contain a large diversity of modified nucleosides;[21] a few of them bear thio functions at the nucleobase. Examples are 2-thiouridine, 4-thiouridine, or 2-thiocytidine including derivatives with various substituents in the 5-position. Nucleosides with thiooxo groups have already been incorporated into artificial DNA, either chemically or by polymerases.[22−25] Consequently, we initiated a study to use these naturally occurring modification sites for oligonucleotide immobilization on gold nanoparticles.

Received: February 3, 2011
Revised: March 8, 2011
Published: March 28, 2011

Scheme 1. Reaction Route for the Formation of Oligonucleotide AuNP Conjugates with Thionucleoside 1 as Anchor Molecule and Proposed Conjugate Structure

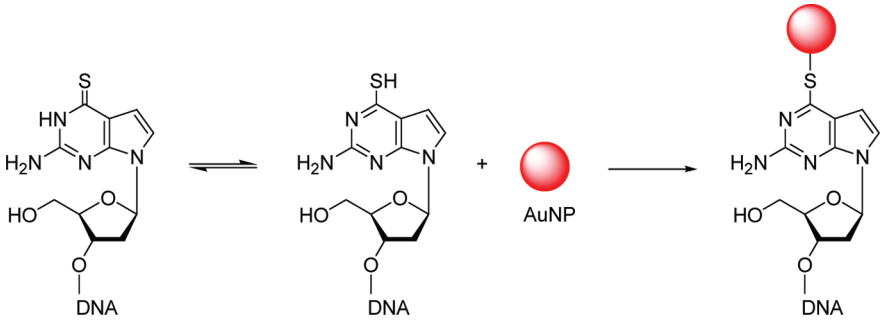

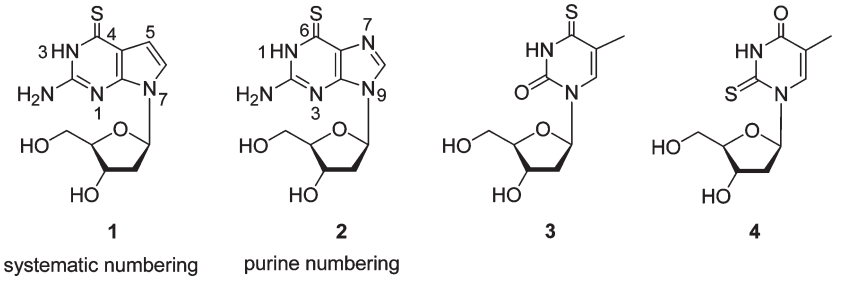

Figure 1. Thionucleosides **1**−**4** employed in this study.

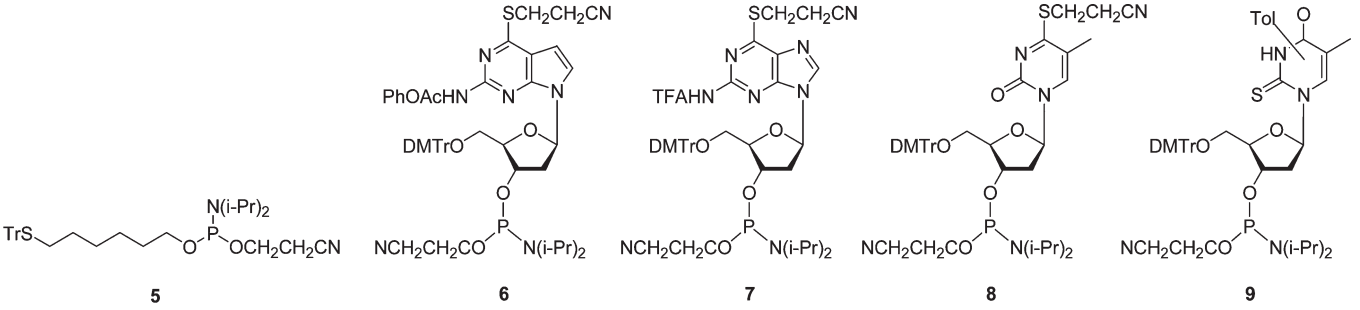

Figure 2. Phosphoramidite building blocks of the hexylthiol linker and the thionucleosides employed for oligonucleotide synthesis.

Herein, we report on a new strategy for conjugation of DNA with gold nanoparticles. In a first step, oligonucleotides are synthesized bearing a thiooxo function ("thio" anchor) at the nucleobase; in a second step, these oligonucleotides are directly attached to the gold surface without prior sulfur protection (Scheme 1). From that background, we selected the four nucleosides 7-deaza-6-thio-2′-deoxyguanosine (**1**), 6-thio-2′-deoxyguanosine (**2**), 4-thio-2′-deoxythymidine (**3**), and 2-thio-2′-deoxythymidine (**4**) for our study as shown in Figure 1. They were introduced into oligonucleotides *via* phosphoramidite chemistry to become an integer part of single-stranded oligonucleotides.

The thiooxo group was utilized as a molecular anchor to gold nanoparticles. First, the stability of the different thiooxonucleosides toward the conditions of solid-phase oligonucleotide synthesis was investigated, and conjugation to the gold surface was tested. Hybridization experiments employing DNA gold nanoparticle conjugates proved the formation of stable DNA-AuNP hybrids with thionucleosides, similar to those linked by conventional protocols.

EXPERIMENTAL PROCEDURES

General Methods and Materials. All chemicals were purchased from Acros, Aldrich, Sigma, or Fluka. The 5′-alkylthiol modifier 6-(triphenylmethyl)-S-$(CH_2)_6$-*O*-2-cyanoethyl diisopropylphosphoramidite (**5**) and phosphoramidites **7**−**9** were obtained from Glen Research (Virginia, USA) (Figure 2). 4-*tert*-Butylphenoxyacetyl protected canonical phosphoramidites were purchased from Millipore (Massachusetts, USA). Solvents were of laboratory grade. Thin-layer chromatography (TLC) was performed on TLC aluminum sheets covered with silica gel 60 F254 (0.2 mm, VWR International, Germany). Flash column chromatography (FC): silica gel 60 (VWR International, Darmstadt, Germany) at 0.4 bar; UV-spectra were recorded on a U-3000 spectrophotometer (Hitachi, Japan); λ_{max} (ε) in nm,

dx.doi.org/10.1021/bc200069j |*Bioconjugate Chem.* 2011, 22, 794–807

ε in $dm^3\ mol^{-1}\ cm^{-1}$. NMR spectra: DPX 300 spectrometer (Bruker, Germany) at 300 MHz for ^1H, 75 MHz for ^{13}C and 121.5 MHz for ^{31}P. The J values are given in Hz; δ values in ppm relative to Me_4Si as internal standard, or 85% H_3PO_4 for ^{31}P. For NMR spectra recorded in DMSO, the chemical shift of the solvent peak was set to 2.50 ppm for ^1H NMR and 39.50 ppm for ^{13}C NMR. Elemental analyses were performed by the Mikroanalytisches Laboratorium Beller, Göttingen, Germany. MALDI-TOF mass spectra were recorded in the linear negative mode with an Applied Biosystems Voyager DE PRO spectrometer with 3-hydroxypicolinic acid (3-HPA) as a matrix. Reversed-phase HPLC was carried out on a 4 × 250 mm RP-18 (10 mm) LiChrospher 100 column (VWR International) with a Merck-Hitachi HPLC pump (model L-6250) connected with a variable wavelength monitor (model 655-A), a controller (model L-500), and an integrator (model D-2500). Melting curves were measured with a Cary-100 Bio UV−vis spectrophotometer (Varian, Australia) equipped with a Cary thermoelectrical controller with a heating rate of 1 °C/min. The T_m values were calculated by *Meltwin 3.0* program. Nanopure water (resistance <0.055 μS/cm) from MembraPure water system (Astacus) was used for all experiments.

*7-(2-Deoxy-β-D-erythro-pentofuranosyl)-2-phenoxyacetamino-7H-pyrrolo[2,3-d]pyrimidin-4(3H)-thione (**10**).* Compound **1**[26] (1.6 g, 5.50 mmol) was dried by repeated coevaporation with anhydrous pyridine (3 × 5 mL), then suspended in pyridine (5 mL). To this solution, trimethylsilyl chloride (3.6 mL, 28.17 mmol) was added at room temperature. After 1 h, phenoxyacetyl chloride (1.1 mL, 7.96 mmol) was introduced, and the solution was stirred at room temperature for another 4 h. The mixture was cooled to 0 °C, diluted with H_2O (5 mL), and stirred for 10 min. Then, aq. ammonia (5 mL) was added, and the solution was stirred for an additional 15 min. The solvent was evaporated to dryness. Purification by FC (silica gel, column 8 × 15 cm, CH_2Cl_2/MeOH, 50:1→25:1) gave **10** as a colorless foam (1.9 g, 81%); mp 205 °C. TLC (CH_2Cl_2/MeOH, 9:1): R_f 0.53. UV λ_{max} (MeOH)/nm 333 (ε/$dm^3\ mol^{-1}\ cm^{-1}$ 47 600). Anal. ($C_{19}H_{20}N_4O_5S$) C, H, N. ^1H NMR (300 MHz, DMSO-d_6): δ = 2.15−2.23 (m, 1H, H_α-2′), 2.38−2.47 (m, 1H, H_β-2′), 3.51−3.54 (m, 2H, H-5′), 3.81−3.84 (m, 1H, H-4′), 4.33−4.36 (m, 1H, H-3′), 4.88 (s, 2H, Pac-CH_2), 4.95 (t, J = 5.3 Hz, 1H, HO-5′), 5.30 (d, J = 3.6 Hz, 1H, HO-3′), 6.41 (m, 1H, H-1′), 6.64 (d, J = 3.7 Hz, 1H, H-5), 6.96−7.01 (m, 3H, phenoxy), 7.29−7.34 (m, 2H, phenoxy), 7.49 (d, J = 3.7 Hz, 1H, H-6), 11.99 (br s, 1H, N−H), 12.89 (br s, 1H, CO-NH).

*4-[(2-Cyanoethyl)thio]-7-(2-deoxy-β-D-erythro-pentofuranosyl)-2-phenoxyacetamino-7H-pyrrolo[2,3-d]pyrimidine (**11**).* 3-Bromopropionitrile (4.0 mL, 48.07 mmol) and anhydrous K_2CO_3 (3.0 g, 21.71 mmol) were added to 25 mL dry DMF and the mixture was stirred vigorously. Compound **10** (1.9 g, 4.45 mmol) was dissolved in 5 mL dry DMF and added dropwise to the stirred solution within 30 min. The reaction mixture was stirred overnight until completion of the reaction (monitored by TLC). The solvent was removed by coevaporation with xylene and the residue was applied to FC (silica gel, column 8 × 15 cm, CH_2Cl_2/MeOH, 500:1→100:1). The main zone yielded **11** as a colorless solid (1.2 g, 55%). TLC (CH_2Cl_2/MeOH, 95:5): R_f 0.22. UV λ_{max} (MeOH)/nm 301 (ε/$dm^3\ mol^{-1}\ cm^{-1}$ 26 700), 244 (73 300). Anal. ($C_{22}H_{23}N_5O_5S$) C, H, N. ^1H NMR (300 MHz, DMSO-d_6): δ = 2.18−2.25 (m, 1H, H_α-2′), 2.50 (m, 1H, H_β-2′), 3.16 (t, 2H, CH_2−CN), 3.51−3.56 (m, 4H, H-5′, H-5″, CH_2−S), 3.84−3.85 (m, 1H, H-4′), 4.36−4.37 (m, 1H, H-3′), 4.94 (t, J = 5.4 Hz, 1H, HO-5′), 5.00 (s, 2H, Pac-CH_2), 5.32 (d, J = 5.3 Hz, 1H, HO-3′), 6.54−6.59 (m, 2H, H-5, H-1′), 6.93−6.98 (m, 3H, phenoxy), 7.28−7.33 (m, 2H, phenoxy), 7.65 (d, J = 3.9 Hz, 1H, H-6), 10.69 (s, 1H, CO-NH).

*4-[(2-Cyanoethyl)thio]-7-[2-deoxy-5-O-(4,4′-dimethoxytrityl)-β-D-erythro-pentofuranosyl]-2-phenoxyacetamino-7H-pyrrolo[2,3-d]pyrimidine (**12**).* Compound **11** (469.5 mg, 1.00 mmol) was coevaporated with anhydrous pyridine (3 × 5.0 mL) and then dissolved in pyridine (5.0 mL). To this solution, 4,4′-dimethoxytriphenylmethyl chloride (440.5 mg, 1.30 mmol) was added and the mixture was stirred at r.t. for 3 h. The reaction was quenched by the addition of MeOH and the mixture was evaporated to dryness. The mixture was subjected to FC (column 4 × 10 cm, elution with CH_2Cl_2/acetone, 20:1) to give **12** as a colorless foam (555.8 mg, 72%). TLC (CH_2Cl_2/MeOH, 95:5): R_f 0.61. UV λ_{max} (MeOH)/nm 302 (ε/$dm^3\ mol^{-1}\ cm^{-1}$ 14 400), 240 (53 500). Anal. ($C_{43}H_{41}N_5O_7S$) C, H, N. ^1H NMR (300 MHz, DMSO-d_6): δ = 2.27−2.31 (m, 1H, H_α-2′), 2.55−2.64 (m, 1H, H_β-2′), 3.13−3.17 (m, 4H, CH_2−CN, H-5′, H-5″), 3.52−3.56 (m, 2H, CH_2−S), 3.71 (s, 6H, OCH_3), 3.95 (m, 1H, H-4′), 4.37 (m, 1H, H-3′), 5.00 (s, 2H, Pac-CH_2), 5.37 (d, J = 4.2 Hz, 1H, HO-3′), 6.52−6.56 (m, 2H, H-5, H-1′), 6.78−7.35 (m, 18H, phenoxy), 7.46 (d, J = 3.6 Hz, 1H, H-6), 10.69 (s, 1H, CO-NH).

*4-[(2-Cyanoethyl)thio]-7-[2-deoxy-5-O-(4,4′-dimethoxytrityl)-β-D-erythro-pentofuranosyl]-2-phenoxyacetamino-7H-pyrrolo-[2,3-d]pyrimidine 3′-[(2-cyanoethyl)-N,N-diisopropylphosphoramidite] (**6**).* Compound **12** (555.8 mg, 0.72 mmol) was dissolved in anhydrous CH_2Cl_2 (3.0 mL) under argon and was reacted with (2-cyanoethyl)diisopropylphosphoramido chloridite (225 μL, 0.95 mmol) in the presence of $^iPr_2EtN$ (220 μL, 1.27 mmol) at room temperature. After 20 min, the reaction mixture was diluted with CH_2Cl_2 and the solution was washed with a 5% aqueous $NaHCO_3$ solution, followed by brine. The organic solution was dried over anhydrous Na_2SO_4, filtered, and concentrated. The residue was subjected to FC (column 4 × 10 cm, CH_2Cl_2/acetone, 25:1) yielding **6** as a colorless foam (429.1 mg, 61%). TLC (CH_2Cl_2/acetone, 95:5): R_f 0.64. ^{31}P NMR (121.5 MHz, $CDCl_3$): δ = 148.56; 148.69.

Hydrolytic Stability of Thiooxonucleosides. The hydrolytic stability of thiooxonucleosides **1**−**4** and **11** under standard deprotection conditions (25% aqueous NH_3, 14−16 h, 60 °C) was monitored by reversed-phase HPLC (RP-18, 250 × 4 mm). Nucleosides **1**−**4** and **11** (about 1 mg) were dissolved in 1 mL of 25% aq. ammonia in a sealed vessel and incubated at 60 °C. After 16 h incubation, aq. ammonia was removed by evaporation and the residue was redissolved in 1 mL HPLC buffer A. 50 μL aliquots of each sample were injected into the HPLC, and the spectra were recorded at 260 nm (for spectra see Supporting Information).

Synthesis, Purification, and Characterization of Oligonucleotides. The syntheses of oligonucleotides were performed on a DNA synthesizer, model 392−08 (Applied Biosystems, Weiterstadt, Germany) at 1 μmol scale. For oligonucleotides containing 7-deaza-6-thio-2′-deoxyguanosine (**1**), 2-thio-2′-deoxythymidine (**4**), or the hexylthiol linker, the corresponding phosphoramidites **5**, **6**, and **9** were used, and the standard synthesis protocol for 3′-(2-cyanoethyl phosphoramidites) was followed.[27] The average coupling yield was always higher than 95%. Oligonucleotides containing the hexylthiol linker, **1** or **4**, were cleaved from solid support with 25% aq. NH_3 and

deprotected for 14−16 h at 60 °C (standard deprotection conditions). Oligonucleotides containing 6-thio-2′-deoxyguanosine (**2**) and 4-thio-2′-deoxythmidine (**3**) were prepared using the corresponding phosphoramidites **7** and **8**, and reagents required for the fast deprotection procedure.[28] For that, 4-*tert*-butylphenoxyacetyl protected canonical phosphoramidites and the capping reagent 4-*tert*-butylphenoxyacetic anhydride instead of acetic anhydride were used. The coupling efficiency was always higher than 95%. Oligonucleotides incorporating **2** or **3** were cleaved from solid support and deprotected in 25% aq. NH_3 solution containing 50 mM NaSH at room temperature overnight (recommended conditions of the supplier). The DMT-containing oligonucleotides were purified on reversed-phase HPLC in the DMT-on modus (Merck-Hitachi-HPLC; RP-18 column) with the following gradient system [A: 0.1 M $(Et_3NH)OAc$ (pH 7.0)/MeCN 95:5; B: MeCN]: 3 min, 20% B in A, 12 min, 20−50% B in A and 25 min, 20% B in A, flow rate 1.0 mL/min. The solvent was evaporated, and the residue was treated with 2.5% $CHCl_2COOH/CH_2Cl_2$ (400 μL) for 5 min at 0 °C to remove the 4,4′-dimethoxytrityl residue. The detritylated oligomers were purified again by reversed-phase HPLC [gradient: 0−20 min 0−20% B in A; flow rate 1 mL/min]. The oligomers were desalted on a short column (RP-18, silica gel) using H_2O for elution of the salt, while the oligomers were eluted with MeOH/H_2O (3:2). The oligonucleotides were lyophilized on a Speed-Vac evaporator to yield colorless solids which were frozen at −24 °C. The 5′-alkylthiol-modified oligonucleotides 5′-d(trityl-S-$(CH_2)_6$-T_{10}-TAG GTC AAT ACT) (**40**) and 5′-d(trityl-S-$(CH_2)_6$-T_{10}-AGT ATT GAC CTA) (**41**) were only purified in the DMT-on modus by reversed-phase HPLC (RP-18) as described above.

The enzymatic hydrolysis of the oligonucleotides was performed as described[29] with snake venom phosphodiesterase (EC 3.1.15.1, *Crotallus adamanteus*) and alkaline phosphatase (EC 3.1.3.1, *Escherichia coli* from Roche Diagnostics GmbH, Germany) in 0.1 M Tris-HCl buffer (pH 8.3) at 37 °C. The hydrolysis product was analyzed by reversed-phase HPLC (RP-18). Quantification of the constituents was made on the basis of the peak areas, which were divided by the extinction coefficients ε_{260} of the nucleosides: dA 15400, dC 7300, dG 11700, dT 8800, 7-deaza-6-thio-2′-deoxyguanosine (**1**) 10100, 6-thio-2′-deoxyguanosine (**2**) 7300, 4-thio-2′-deoxythymidine (**3**) 1500. MALDI-TOF mass spectra were recorded in the linear negative mode with an Applied Biosystems Voyager DE PRO spectrometer with 3-hydroxypicolinic acid (3-HPA) as a matrix. The detected masses were identical with the calculated values (see Supporting Information).

General Procedure for the Preparation of Oligonucleotide Gold Nanoparticle Conjugates Employing Thiooxonucleosides as Molecular Anchor. The gold nanoparticle solution (15 nm particle diameter) was prepared from a $HAuCl_4$ solution by citrate reduction according to the protocol originally reported by Turkevitch[30] and later described by Letsinger and Mirkin.[13] The nanoparticle concentration was determined by UV/vis using $\varepsilon_{520} = 4.2 \times 10^8\ M^{-1}\ cm^{-1}$ (UV/vis_{max}: 520 nm).[31] The gold nanoparticles (~3 nM) were functionalized with oligonucleotides **18**−**29** and **36**−**39** containing thiooxonucleosides **1**−**4** at different positions within their sequences. The DNA-AuNP conjugates **Au18**-**Au29** and **Au36**-**Au39** were prepared by mixing 1 mL of the respective AuNP solution with the aq. solution of the purified oligonucleotide (1−5 μL) to yield a final oligonucleotide concentration of 3 μM. The coupling reaction was performed at slightly elevated temperature (40 °C). After standing for 20 h, 5 μL of a 2 M NaCl, 0.2 mM phosphate buffer solution (pH 7.0) was added under constant stirring to bring the colloidal solutions to a 0.01 M NaCl concentration. The solution was allowed to stand for 6−8 h. The NaCl concentration was increased stepwise using 2 M NaCl and 0.2 mM phosphate buffer solution (pH 7.0). First, the colloids were salted to 0.02 M NaCl and allowed to age for another 6−8 h, then salted to 0.05 M NaCl with 6−8 h of incubation, and were finally salted to 0.1 M NaCl. Subsequently, the DNA gold nanoparticle solutions were centrifuged (8000 rpm, 45 min) and the clear supernatant was taken off to remove unbound oligonucleotides. The precipitate was redispersed in 1 mL of a 0.1 M NaCl, 10 mM phosphate buffer solution (pH 7.0). After incubation (24 h, 40 °C), the conjugate solutions were centrifuged and washed again with the same buffer, finally yielding 1 mL of the DNA-AuNP conjugates **Au18**-**Au29** and **Au36**-**Au39** (Table 1). The DNA-AuNP conjugates were characterized by UV/vis spectroscopy and stored at 4 °C.

Table 1. Gold Nanoparticle Conjugates Immobilizing an Arbitrary Number of Oligonucleotides and the Maximum of VIS Absorption[a]

Oligonucleotide Gold Nanoparticle Conjugates	Max. VIS Absorption [nm]
5′-d(**1** T_{10} TAG GTC AAT ACT) (**Au18**)	524
5′-d(**1** T_{10} AGT ATT GAC CTA) (**Au19**)	524
5′-d(**2** T_{10} TAG GTC AAT ACT) (**Au20**)	524
5′-d(**2** T_{10} AGT ATT GAC CTA) (**Au21**)	524
5′-d(**3** T_{10} TAG GTC AAT ACT) (**Au22**)	524
5′-d(**3** T_{10} AGT ATT GAC CTA) (**Au23**)	524
5′-d(**4** T_{10} TAG GTC AAT ACT) (**Au24**)	524
5′-d(**4** T_{10} AGT ATT GAC CTA) (**Au25**)	524
5′-d(**11** T_{10} AGT ATT GAC CTA) (**Au26**)	526
5′-d(**11** T_{10} AGT ATT GAC CTA) (**Au27**)	526
5′-d(**111** T_{10} TAG GTC AAT ACT) (**Au28**)	526
5′-d(**111** T_{10} AGT ATT GAC CTA) (**Au29**)	525
5′-d(TA**1** GTC AAT ACT TAG GTC AAT ACT) (**Au36**)	526
5′-d(A**1**T ATT GAC CTA AGT ATT GAC CTA) (**Au37**)	525
5′-d(TAG GTC AAT ACT TA**1** GTC AAT ACT) (**Au38**)	524
5′-d(AGT ATT GAC CTA A**1**T ATT GAC CTA) (**Au39**)	525
5′-d(**S**-$(CH_2)_6$-T_{10} TAG GTC AAT ACT) (**Au40**)	523
5′-d(**S**-$(CH_2)_6$-T_{10} AGT ATT GAC CTA) (**Au41**)	523

[a] Spacer T_{10} = 5′-d(TTT TTT TTT T).

Scheme 2. Synthesis of Phosphoramidite Building Block 6[a]

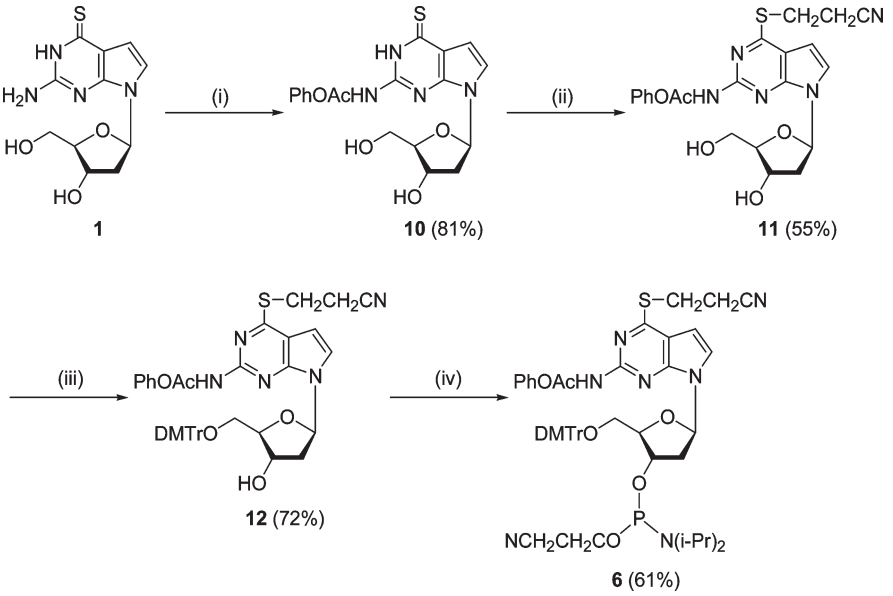

[a] Reagents and conditions: (i) Me_3SiCl, phenoxyacetyl chloride, pyridine, aq. NH_3, 4 h, r.t.; (ii) 3-bromopropionitrile, anh. K_2CO_3, DMF, overnight, r.t.; (iii) DMTr-Cl, pyridine, 3 h, r.t.; (iv) (2-cyanoethyl)diisopropylphosphoramido chloridite, *N*,*N*-diisopropylethylamine, anh. CH_2Cl_2, 20 min, r.t.

All conjugates show plasmon resonance at around 524 nm indicating a nonaggregated state (Table 1 and Supporting Information).

Preparation of DNA-AuNP Conjugates Employing the Hexylthiol Linker As Anchoring Site. DNA-AuNPs employing oligonucleotides with terminal alkylthiol linkers were prepared by a protocol reported previously.[13,32] The DNA-AuNP conjugates **Au40** and **Au41** were characterized by UV/vis spectroscopy showing plasmon resonance at 523 nm which is correlated to a nonaggregated state (for spectra, see Figure S2, Supporting Information).

Scanning Electron Microscopy (SEM). A typical sample was prepared by dropping a DNA-AuNP conjugate into a silicon wafer which was then subsequently dried and imaged.

RESULTS AND DISCUSSION

The conventional protocol for the attachment of oligonucleotides onto gold nanoparticle surfaces makes use of oligonucleotides modified at their 5′- or 3′-termini by an alkylthiol linker.[5,12−14,32−34] However, this protocol is laborious and accompanied by drawbacks to form SH-modified oligonucleotides ready for immobilization. This includes (i) the detritylation of the protected thiol-group with silver nitrate, (ii) removal of excess silver nitrate and (iii) desalting of the free thiol-modified oligonucleotides. Furthermore, the immobilization of the reactive oligonucleotides to the gold nanoparticles has to be performed shortly after preparation to reduce unwanted side reactions (e.g., disulfide formation). Moreover, silver ions or metallic silver which can bind to both oligonucleotides and gold nanoparticles are difficult to remove quantitatively.

In this study, we made use of the sulfur atom of thiooxonucleosides to conjugate oligonucleotides to gold nanoparticles. The sulfur atom of these nucleosides is expected to bind to the gold surface *via* the thiooxo group or the corresponding mercapto group. Recently, the triphosphate of 4-thio-2′-deoxythymidine was incorporated enzymatically into DNA, and the sulfur functionality was used to attach the DNA oligonucleotides to gold electrodes.[35,36] For our study, we selected the thiooxonucleosides **1**−**4** for incorporation into oligonucleotides *via* phosphoramidite chemistry. In this respect, the stability of **1**−**4** against nucleophilic sulfur displacement under alkaline deprotection conditions was investigated. Thiooxonucleosides **1**−**4** were used as a molecular anchor to the gold nanoparticle surface and their capability to form DNA-AuNPs was evaluated.

Building Block Synthesis. The phosphoramidites **5**−**9** were selected for oligonucleotide syntheses (Figure 2). Compounds **5** and **7**−**9** are commercially available, while phosphoramidite **6** has to be synthesized using nucleoside **1** as starting material.[26]

For the protection of the amino group, the phenoxyacetyl residue[37] was chosen, and the protocol of transient protection (→ **10**, 81% yield) was used (Scheme 2). The thiooxo function was protected with the cyanoethyl group (→ **11**, 55% yield) as described for the parent purine compound **2**.[38] The protected intermediate **11** was converted into the 5′-*O*-DMT derivative **12** under standard conditions. Phosphitylation with 2-cyanoethyl-*N*,*N* diisopropyl-phosphoramidochloridite furnished the phosphoramidite **6** (61% yield, Scheme 2).

All compounds were characterized by UV-spectra and ^{1}H- and ^{13}C NMR spectra as well as by elemental analysis (Table 2 and Experimental Procedures section). The assignments of ^{13}C NMR chemical shifts of the sugar moiety and the protecting groups were made on the basis of ^{1}H−^{13}C gated-decoupled spectra (for more data, see Supporting Information) in combination with already published data.[38] For 7-deaza-6-thio-2′-deoxyguanosine (**1**), the chemical shifts for C2 and C6 were only assigned tentatively.[38] Therefore, now we used the deuterium isotope upfield shift approach to assign the carbon-2 signal,[39,40] which is directly connected with the amino group. In a DMSO solution, containing a H_2O/D_2O mixture, the carbon-2 signal is split into two singlets (Figure S6, Supporting Information): the original one and one which is shifted 0.04 ppm upfield. Consequently, C2 was assigned to the 152.2 ppm signal and C6 to the 175.7 ppm signal (Table 2).

dx.doi.org/10.1021/bc200069j |*Bioconjugate Chem.* 2011, 22, 794–807

Table 2. ^{13}C-NMR Chemical Shifts (δ) of 7-Deaza-6-thio-2′-deoxyguanosine Derivatives[a]

	C(2)[b]	C(4)[b]	C(4a)[b]	C(5)[b]	C(6)[b]	C(7a)[b]					
compd	C(2)[c]	C(6)[c]	C(5)[c]	C(7)[c]	C(8)[c]	C(4)[c]	C(1′)	C(2′)	C(3′)	C(4′)	C(5′)
c^7G_d[e]	152.5	158.5	100.1	102.1	116.7	150.5	82.2	39.5	70.8	86.9	61.9
1	152.2	175.7	113.1	104.4	120.2	147.1	82.2	-[d]	70.9	87.1	61.9
10	145.4	174.8	116.8	104.7	122.7	143.4	82.5	-[d]	70.6	87.1	61.5
11	151.0	167.3	119.5	99.5	125.0	149.2	82.6	-[d]	70.9	87.4	61.8
12	151.1	167.3	119.4	99.5	124.8	149.2	82.7	-[d]	70.7	85.5	64.2

[a] Measured in DMSO-d_6 at 298 K. [b] Systematic numbering. [c] Purine numbering. [d] Superimposed by the DMSO signal. [e] c^7G_d: 7-deaza-2′-deoxyguanosine; ^{13}C NMR chemical shifts taken from ref 41.

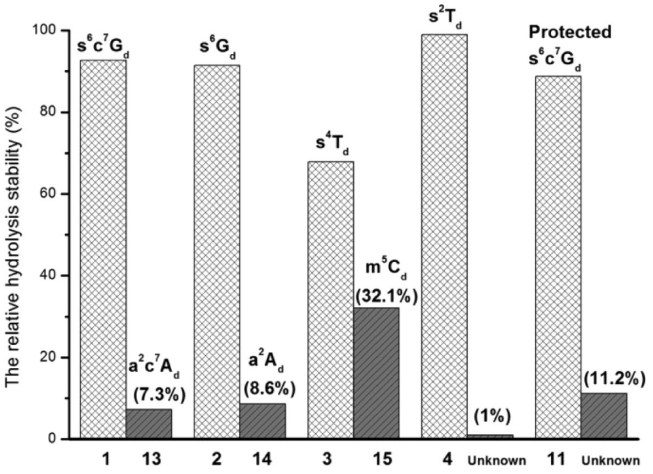

Figure 3. Graph showing the alkaline hydrolysis stability of thiooxonucleosides **1**−**4** and protected **11**. After incubation in a solution of 25% aq. NH_3 at 60 °C for 16 h, compounds **1**−**4** and **11** were analyzed by reversed-phase HPLC at 260 nm. Relative quantification was calculated on the basis of peak areas which were divided by the extinction coefficient (ε_{260}) of the respective nucleoside (for details see Supporting Information). $s^6c^7G_d$: 7-deaza-6-thio-2′-deoxyguanosine (**1**), $a^2c^7A_d$: 2-amino-7-deaza-2′-deoxyadenosine (**13**), s^6G_d: 6-thio-2′-deoxyguanosine (**2**), a^2A_d: 2-amino-2′-deoxyadenosine (**14**), s^4T_d: 4-thio-2′-deoxythymidine (**3**), m^5C_d: 5-methyl-2′-deoxycytidine (**15**), s^2T_d: 2-thio-2′-deoxythymidine (**4**), **11**: 6-[(2-cyanoethyl)thio]-2-phenoxyacetamino-7-deaza-2′-deoxyguanosine.

Moreover, compared to the parent nucleoside 7-deaza-2′-deoxyguanosine (c^7G_d; Table 2), the sulfur atom of thionucleoside **1** attached to carbon-6—instead of the oxygen atom of c^7G_d—induces a significant downfield shift of 17.2 ppm on C6.

Stability of Thiooxonucleosides 1−4 toward Alkaline Hydrolysis. Prior to oligonucleotide synthesis, the stability of the thiooxo group of nucleosides **1**−**4** toward the standard oligonucleotide deprotection conditions (25% aq. NH_3, 16 h, 60 °C) was investigated. This study was motivated by earlier reports on sulfur-amino group exchanges of 6-thio-2′-deoxyguanosine (**2**) (→ 2-amino-2′-deoxyadenosine, **14**)[24] and 4-thio-2′-deoxythymidine (**3**) (→ 5-methyl-2′-deoxycytidine, **15**)[42] under alkaline conditions. Moreover, the unknown compound **11** employing a cyanoethyl protecting group at the sulfur function and a 2-phenoxyacetamino group was also subject of this study. With this experiment, we intended to confirm the applicability of the cyanoethyl protecting group at sulfur-6 under standard oligonucleotide deprotection conditions and conversion to the desired 7-deaza-6-thio-2′-deoxyguanosine (**1**).

Thus, nucleosides **1**−**4** and **11** were incubated in 25% aq. NH_3, 16 h, 60 °C (standard oligonucleotide deprotection conditions) and analyzed by reversed-phase HPLC at 260 nm. Byproducts were identified by coelution with authentic nucleosides (for experimental procedure and HPLC profiles, see the Supporting Information).

The thiooxo group at position-6 of purine nucleosides or position-2 of pyrimidine nucleosides is considerably more stable compared to position-4 of pyrimidine nucleosides. Accordingly, among nucleosides **1**−**4**, the thiooxo group of 4-thio-2′-deoxythymidine (**3**) is the most labile one toward the standard oligonucleotide deprotection conditions (32% conversion to 5-methyl-2′-deoxycytidine, **15**). On the contrary, the thiooxo group of 2-thio-2′-deoxythymidine (**4**) was the most stable one, and less than 1% conversion into an unidentified product was detected (Figure 3 and Supporting Information). The thiooxo groups of the purine and 7-deazapurine nucleosides **1** and **2** showed similar stabilities (**1**: 7% conversion, **2**: 9% conversion, Figure 3). For the protected compound **11**, conversion into an unidentified side product amounts to 11% which is within the same range as for nucleosides **1** and **2**. However, it should be noted that, for **11**, the stability of the sulfur function is related to deprotection and conversion from 6-cyanoethyl(thio) into the desired 6-sulfur group (Figure 3 and Supporting Information). From the above-described experiments, the following order of stability of the thiooxo groups of nucleosides **1**−**4** and **11** toward alkaline hydrolysis (25% aq. NH_3, 16 h, 60 °C) was deduced: **4** > **1** > **2** > **11** > **3** (Figure 3).

Oligonucleotide Synthesis and Characterization. With the informations of the alkaline hydrolysis experiments in hand, a series of unmodified and modified oligonucleotides (**16**−**39**) containing thiooxonucleosides **1**−**4** at different positions were synthesized on solid phase at 1 μmol scale (Table 4), and the accessibility of pure oligomers was studied. Two different protocols of oligonucleotide syntheses were employed: (i) oligonucleotide synthesis using fast deprotectable building blocks and (ii) standard oligonucleotide synthesis employing standard building blocks. Oligonucleotides incorporating 4-thio-2′-deoxythymidine (**3**) or 6-thio-2′-deoxyguanosine (**2**) were synthesized under conditions already reported in the literature utilizing phosphoramidites **7** and **8** which are suitable for fast deprotection conditions.[38,43] Oligonucleotides were cleaved from solid support and deprotected in a 25% aq. NH_3 solution containing 50 mM NaSH at room temperature overnight. Sulfur exchange was avoided by employing the protocol of fast deprotection[28] and the presence of sodium hydrogensulfide. In contrast, oligonucleotides containing 2-thio-2′-deoxythmidine (**4**) or 7-deaza-6-thio-2′-deoxyguanosine (**1**) were synthesized and deprotected

dx.doi.org/10.1021/bc200069j |Bioconjugate Chem. 2011, 22, 794–807

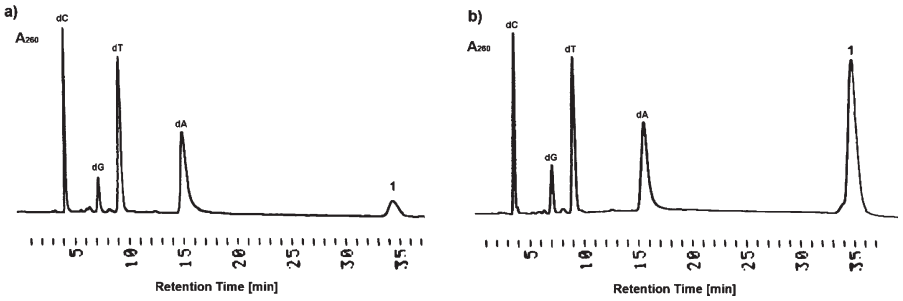

Figure 4. HPLC elution profiles of (a) the enzymatic hydrolysis products of oligonucleotide **30** obtained after hydrolysis with snake venom phosphodiesterase and alkaline phosphatase in 0.1 M Tris−HCl buffer (pH 8.5) at 37 °C and (b) the artifical mixture of the hydrolysis products of oligonucleotide **30** and thiooxonucleoside **1**. Column: RP-18 (200 × 10 mm); gradient [A: 0.1 M (Et_3NH)OAc (pH 7.0)/MeCN 95:5]: 100% A; flow rate: 0.7 mL/min.

under standard conditions (25% aq. NH_3, 14−16 h, 60 °C) in the absence of sodium hydrogensulfide. The oligonucleotides were isolated and purified by reversed-phase HPLC (for details see Experimental Procedures).

The nucleobase composition of the modified oligonucleotides was also confirmed by tandem enzymatic hydrolysis with snake-venom phosphodiesterase (EC 3.1.15.1, *Crotallus adamanteus*) followed by alkaline phosphatase (EC 3.1.3.1, *Escherichia coli*) in 0.1 M Tris-HCl buffer (pH 8.5) at 37 °C as described previously.[29] As an example, the HPLC profiles of the nucleoside composition of oligonucleotide **30** after enzymatic hydrolysis (Figure 4a) and the artificial mixture of the hydrolysis products of **30** and nucleoside **1** (Figure 4b) are shown depicting the correct nucleobase composition of the oligonucleotide.

Both MALDI-TOF mass spectrometry (Supporting Information, Table S1) and enzymatic hydrolysis confirm that deprotection of oligonucleotides containing **1** under standard conditions (25% aq. NH_3, 14−16 h, 60 °C) yields the desired 7-deaza-6-thio-2′-deoxyguanosine (**1**) as constituent of the respective oligonucleotides, as no significant side products pointing toward sulfur exchange were detected. These findings make **1** highly advantageous over its purine congener **2** from which severe side product formation was reported when treated under these conditions.[38]

A problem associated with oligonucleotides containing thionucleosides is disulfide formation leading to cross-linked oligonucleotides. Manuscripts reporting on interstrand cross-linking through thionucleosides describe template directed protocols and the application of mild oxidants to achieve disulfide formation.[44,45] In addition, according to Waters and Connolly,[24] disulfide formation is only observed when oligonucleotides are kept in aqueous solution at neutral pH values at room temperature. Therefore, to avoid disulfide formation, we always stored our oligonucleotides as dry material at −20 °C. Throughout synthesis, purification, and characterization of oligonucleotides incorporating thionucleosides **1**−**4**, we did not make any observations indicating cross-linking of oligonucleotides due to disulfide formation. As mentioned above, in all cases, the detected masses of oligonucleotides were identical with the calculated values (Supporting Information, Table S1). Moreover, it should be noted that covalent binding to AuNPs can be achieved *via* thiol groups as well as disulfides.[17,46]

Preparation of Oligonucleotide Gold Nanoparticle Conjugates. Next, the applicability of thionucleosides **1**−**4** as components of single-stranded oligonucleotides was evaluated for nanoparticle conjugation. Selected key properties of the corresponding DNA-AuNP conjugates, such as stability in the presence of NaCl, UV/vis absorption maximum, and the ability to hybridize with complementary conjugates, were compared to DNA-AuNP conjugates utilizing the 5′-hexylthiol linker as molecular anchor.

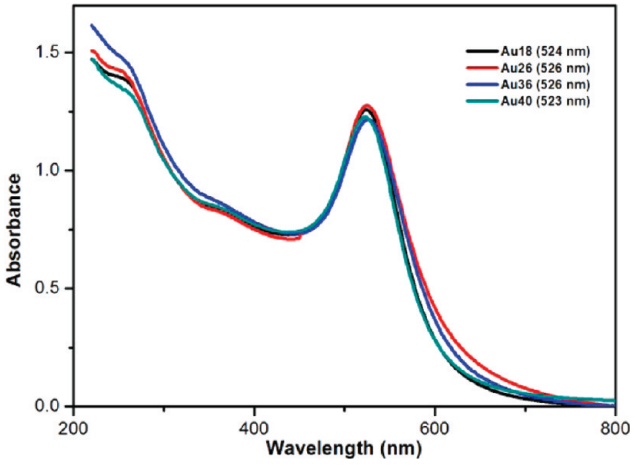

Figure 5. UV/vis profiles of selected DNA-AuNP conjugates in 0.1 M NaCl, 10 mM phosphate buffer, pH 7.0.

The unmodified AuNPs were functionalized with oligonucleotides **18**−**39** containing one or multiple thiooxonucleosides (**1**−**4**) at different positions. For that, 1 mL of the unmodified AuNP solution was mixed with the aqueous solution of the respective purified oligonucleotide (1−5 μL) to yield a final oligonucleotide concentration of 3 μM. The conjugation was performed at slightly elevated temperature (40 °C). The NaCl concentration of the DNA-AuNP solution was increased stepwise with phosphate buffer (2 M NaCl, 0.2 mM phosphate buffer, pH 7.0) to a final NaCl concentration of 0.1 M. Unbound oligonucleotides were removed from the DNA-AuNP solutions by a repeated washing and centrifugation protocol with 0.1 M NaCl, 10 mM phosphate buffer (pH 7.0) (for details see Experimental Procedures). During the whole procedure, the DNA gold nanoparticle solutions stayed deep red in color. However, we found that the preparation of DNA-AuNP conjugates with oligonucleotides **20**−**21** or **24**−**25** incorporating **2** and **4** were encountered with difficulties. Contrary to all other samples, conjugation of **20**−**21** and **24**−**25** to AuNPs failed several times (50% failure). Moreover, the centrifugation speed had to be reduced significantly from 8000 rpm (standard speed) to 5800 rpm; otherwise, it was not possible to redisperse the precipitate. Finally, all DNA-AuNP

Table 3. Applicability of Thiooxonucleosides 1−4 and 5′-Hexylthiol Linker for Gold Nanoparticle Conjugate Formation[e]

Entry	Nucleoside	Conjugate 5'-d(**X** T_{10} TAG GTC AAT ACT)	Conjugate 5'-d(**X** T_{10} AGT ATT GAC CTA)	Hybridization Capability
1	**X = 1**	**Au18**: yes[a,b]	**Au19**: yes[a,b]	yes
2	**X = 2**	**Au20**: yes[a,b]	**Au21**: yes[a,b]	yes[d]
3	**X = 3**	**Au22**: yes[a] / no[b]	**Au23**: yes[a] / no[b]	yes
4	**X = 4**	**Au24**: yes[a] / no[b]	**Au25**: yes[a] / no[b]	no
5	**X = 5**	**Au40**: yes[a,b]	**Au41**: yes[a,b]	yes

[a] Stable oligonucleotide gold nanoparticle conjugates were obtained in 0.1 M NaCl, 10 mM phosphate buffer, pH 7.0. [b] Stable oligonucleotide gold nanoparticle conjugates were obtained in 0.2 M NaCl, 10 mM phosphate buffer, pH 7.0. [c] The hybridization experiment was performed in 0.1 M NaCl, 10 mM phosphate buffer, pH 7.0 with overnight incubation time. [d] Formation of the DNA gold nanoparticle network occurred much more slowly and required several days. Spacer T_{10} = 5′-d(TTT TTT TTT T). [e] Red ball = 15-nm-diameter gold nanoparticle.

Table 4. T_m Values and Thermodynamic Data of Oligonucleotide Duplexes Containing Thiooxonucleosides 1−4 as Overhanging Ends or Opposite Canonical Nucleosides[a,b]

duplex		T_m [°C]	ΔT_m [°C][c]
5′-d(TAG GTC AAT ACT) 3′-d(ATC CAG TTA TGA)	(16) (17)	47	-
5′-d(**1** T_{10} TAG GTC AAT ACT) 3′-d(ATC CAG TTA TGA T_{10} **1**)	(18) (19)	48	+1
5′-d(**2** T_{10} TAG GTC AAT ACT) 3′-d(ATC CAG TTA TGA T_{10} **2**)	(20) (21)	47	0
5′-d(**3** T_{10} TAG GTC AAT ACT) 3′-d(ATC CAG TTA TGA T_{10} **3**)	(22) (23)	47	0
5′-d(**4** T_{10} TAG GTC AAT ACT) 3′-d(ATC CAG TTA TGA T_{10} **4**)	(24) (25)	47	0
5′-d(**11** T_{10} TAG GTC AAT ACT) 3′-d(ATC CAG TTA TGA T_{10} **11**)	(26) (27)	47	0
5′-d(**111** T_{10} TAG GTC AAT ACT) 3′-d(ATC CAG TTA TGA T_{10} **111**)	(28) (29)	47	0
5′-d(TAG GTC AAT ACT) 3′-d(ATC CAG TTA T**1**A)	(16) (30)	43	−4
5′-d(TAG GTC AAT ACT) 3′-d(ATC CA**1** TTA TGA)	(16) (31)	40	−7
5′-d(TA**11**TC AAT ACT) 3′-d(ATC CA**1** TTA T**1**A)	(32) (33)	17	−30
5′-d(TAG GTC AAT ACT TAG GTC AAT ACT) 3′-d(ATC CAG TTA TGA ATC CAG TTA TGA)	(34) (35)	65	-
5′-d(TA**1** GTC AAT ACT TAG GTC AAT ACT) 3′-d(ATC CAG TTA TGA ATC CAG TTA T**1**A)	(36) (37)	55	−10
5′-d(TAG GTC AAT ACT TA**1** GTC AAT ACT) 3′-d(ATC CAG TTA T**1**A ATC CAG TTA TGA)	(38) (39)	53	−12

[a] Measured at 260 nm in 0.1 M NaCl, 10 mM phosphate buffer (pH 7.0), with 5 μM single-strand concentration. [b] Spacer T_{10} = 5′-d(TTT TTT TTT T). [c] ΔT_m was calculated as $T_m^{\text{base mismatch}} - T_m^{\text{base match}}$.

conjugates **Au18**-**Au29** and **Au36**-**Au39** showed the expected plasmon resonance at around 524 nm indicating a nonaggregated state (Table 1, Figure 5, and Figure S2, Supporting Information). It is worthwhile to mention that the same absorption maximum (524 nm) is also observed for DNA-AuNP conjugates **Au36**-**Au39**, in which the attachment succeeds through thionucleoside **1** situated within an internal position of the respective oligonucleotide (Figure 5). Thus, it can be concluded that thionucleoside **1** can also function as a molecular anchor for AuNPs through an internal position of an oligonucleotide.

For comparison, oligonucleotides **40** and **41** incorporating a 5′-hexylthiol linker were conjugated to AuNPs (→ **Au40**, **Au41**; Table 1) employing the conventional protocol reported earlier by others.[47] The UV/vis spectra of DNA-AuNP conjugates **Au40** and **Au41** show a plasmon resonance at 523 nm (Table 1, Figure 5).

Next, the stability of DNA-AuNP conjugates **Au18**-**Au29** containing the different thiooxonucleosides **1**−**4** and **Au40**, **Au41** employing the hexylthiol linker was evaluated at higher salt concentration (0.2 M NaCl, 10 mM phosphate, pH 7.0 buffer solution). For that, UV/vis spectra of the DNA-AuNP conjugate solutions were recorded at different time intervals and compared (for UV/vis profiles at the different time intervals see the Supporting Information, Figure S3). This experiment was performed to provide more information on the applicability of **1**−**4** for AuNP conjugation and hence on the stability of the different conjugates (Table 3). The DNA-AuNP conjugates **Au22**-**Au25** using 4-thio-2′-deoxythymidine (**3**) or 2-thio-2′-deoxythymidine (**4**) as anchor molecules were unstable in the presence of higher NaCl concentration. This became immediately evident for DNA-AuNPs **Au24** and **Au25** containing 2-thio-2′-deoxythymidine (**4**), due to aggregation of the DNA-AuNPs (solutions turned black) followed by precipitation (Table 3, entry 4), whereas DNA-AuNPs **Au22** and **Au23** showed partial precipitation which was deduced from a significant decrease in the maximum of the UV/vis absorption profile (36%) after overnight incubation compared to the original profile (0 h incubation) (Figure S3, Supporting Information). However, the plasmon resonance of conjugates **Au22** and **Au23** was almost unchanged (524.5 nm), but the red color of the solutions was much fainter compared to the original solutions. According to these observations, we classified DNA-AuNP conjugates using 4-thio-2′-deoxythymidine (**3**) as anchor molecule (**Au22** and **Au23**) as not stable in the presence of higher NaCl concentration (see Table 3, entry 3).

dx.doi.org/10.1021/bc200069j |*Bioconjugate Chem.* 2011, 22, 794–807

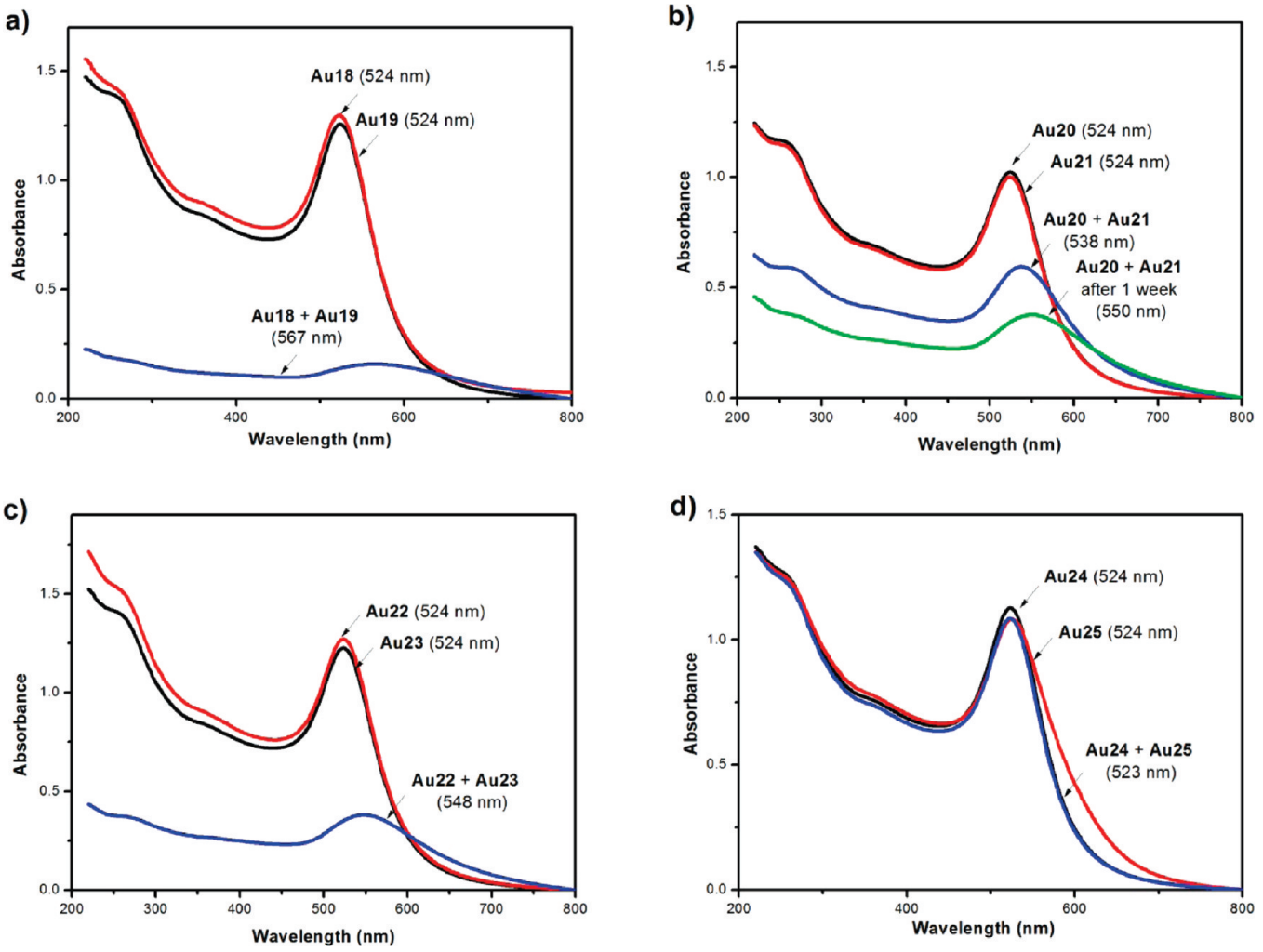

Figure 6. UV/vis spectra of (a) DNA-AuNP conjugates **Au18**, **Au19** using 7-deaza-6-thio-2′-deoxyguanosine (**1**) as anchor, and the DNA-AuNP network **Au18•Au19** formed after overnight incubation (blue curve). (b) DNA-AuNP conjugates **Au20** and **Au21** using 6-thio-2′-deoxyguanosine (**2**) as anchor (red and black curves), the DNA-AuNP network **Au20•Au21** formed after overnight incubation (blue curve) and after several days of incubation (green curve). (c) DNA-AuNP conjugates **Au22** and **Au23** using 4-thio-2′-deoxythymidine (**3**) as anchor and the DNA-AuNP network formed by **Au22•Au23** after overnight incubation (blue curve). (d) DNA-AuNP conjugates **Au24** and **Au25** using 2-thio-2′-deoxythymidine (**4**) as anchor (red and black curves) and after overnight incubation (blue curve).

On the contrary, the DNA-AuNPs **Au18**-**Au21** using 7-deaza-6-thio-2′-deoxyguanosine (**1**) or 6-thio-2′-deoxyguanosine (**2**) as conjugation site (Table 3, entry 1−2) and **Au40**, **Au41** making use of a hexylthiol linker (Table 3, entry 5) were of comparable stability, and all conjugates were significantly more stable than **Au22**-**Au25** under the higher salt concentration (see also Supporting Information, Figure S3).

Similar results were found for DNA-AuNP conjugates **Au26**-**Au29** having consecutive 7-deaza-6-thio-2′-deoxyguanosine (**1**) modifications at the 5′-end of oligonucleotides **26**−**29**, after overnight incubation in 0.2 M NaCl, 10 mM phosphate, pH 7.0 buffer solution (data not shown).

Duplex Stability of Oligonucleotides Containing Thiooxonucleosides 1−4 and Oligonucleotide Gold Nanoparticle Conjugates. It is well-known that in thiooxonucleosides the replacement of the oxygen atom by sulfur leads to a destabilization of duplex DNA since the thio group is a poorer hydrogen bond acceptor than the normal carbonyl, and bulkiness of the sulfur atom can interfere with hybridization.[48]

For clarification, hydridization studies were performed with non-immobilized oligonucleotide duplexes incorporating compounds **1**−**4** (Table 4). Single or multiple thiooxonucleosides (**1**−**4**) were incorporated as overhanging ends together with a 5′-d$(T)_{10}$ spacer. Table 4 shows that all duplexes have similar T_m values (47 °C) as the parent unmodified duplex 5′-d(TAG GTC AAT ACT) (**16**) • 3′-d(ATC CAG TTA TGA) (**17**).

As 7-deaza-6-thio-2′-deoxyguanosine (**1**) has not been incorporated into oligonucleotides before, its properties as a constituent of duplex DNA were investigated in more detail. Thus, consecutive and random positions have been selected for modification with **1**, and T_m values were determined.

A single replacement of nucleoside **1** in the center or at the periphery of the 12-mer duplex reduced the stability of the duplex. The effect was more pronounced when **1** was incorporated in the center of the oligonucleotide duplex (**16•31**: $\Delta T_m = -7$ °C) than at the periphery (**16•30**: $\Delta T_m = -4$ °C). Multiple modifications led to a significant further destabilization ($\Delta T_m = -30$ °C for **32•33**) (Table 4). Consistently, two

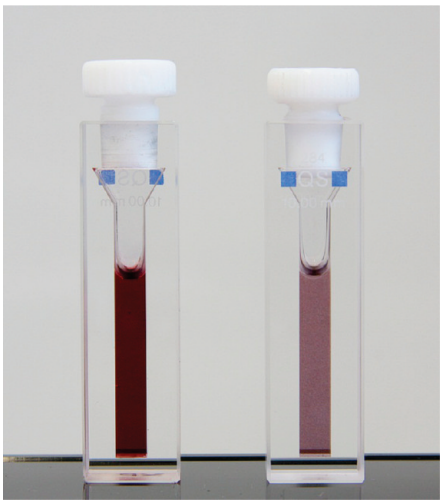

Figure 7. Left cuvette: unmodified deep red gold nanoparticle solution. Right cuvette: purple DNA-AuNP conjugate solution after assembly of **Au18•Au19** (12 h incubation, the sample is shown after intensive shaking).

incorporations of nucleoside **1** within the center or at the periphery of 24-mer duplexes (**36•37**, **38•39**) lead to a strong decrease of the duplex stability when compared to the parent unmodified duplex **34•35** ($\Delta T_m = -10$ °C for **36•37** and $\Delta T_m = -12$ °C for **38•39**). As can be seen from Table 4, 7-deaza-6-thio-2′-deoxyguanosine (**1**) has a strong destabilizing effect on duplex stability similar to that reported for the parent 6-thio-2′-deoxyguanosine (**2**).[48]

Next, hybridization experiments were performed with oligonucleotide gold nanoparticle conjugates. In a typical experiment, two DNA-AuNP conjugates carrying oligonucleotides with complementary sequences were mixed together (equal concentrations), e.g., DNA-AuNP conjugates **Au18** and **Au19** using 7-deaza-6-thio-2′-deoxyguanosine (**1**) as molecular anchor. After incubation overnight at 5 °C, the propensity of hybridization was evaluated by UV/vis measurements. Almost all complementary DNA-AuNP conjugates show hybridization evidenced by slow red shifting and broadening of the plasmon resonance band (Table 3 and Figures 6, 7) with the exception of the complementary conjugates **Au24** and **Au25** which utilize 2-thio-2′-deoxythymidine (**4**) as molecular anchor.

In the case of the complementary conjugates **Au18•Au19**, **Au22•Au23**, and **Au40•Au41**, hybridization led to the formation of a DNA gold nanoparticle network which precipitated from solution (→ dark red precipitate with a clear supernatant) within one night. After intensive shaking of the DNA-AuNP solution, the precipitate can be redispersed leading to a purple solution with UV/vis maxima of 567 nm for **Au18•Au19** (Figure 6a), 548 nm for **Au22•Au23** (Figure 6c), and 554 nm for **Au40•Au41** (spectra not shown).

On the contrary, the UV/vis spectrum of the DNA-AuNP solution containing the complementary conjugates **Au20** and **Au21**, which use 6-thio-2′-deoxyguanosine (**2**) as molecular anchor, shows only a moderate red shift (524 nm→538 nm) of the plasmon resonance band accompanied by a smaller decrease of the absorption and only a slight broadening of the plasmon resonance band (Figure 6b, blue curve). However, no precipitation of the DNA-AuNPs was observed after incubation overnight. Prolonged incubation of about 1 week finally led to the precipitation of the DNA gold nanoparticle network. After intensive shaking of the DNA-AuNP solution **Au20•Au21**, the

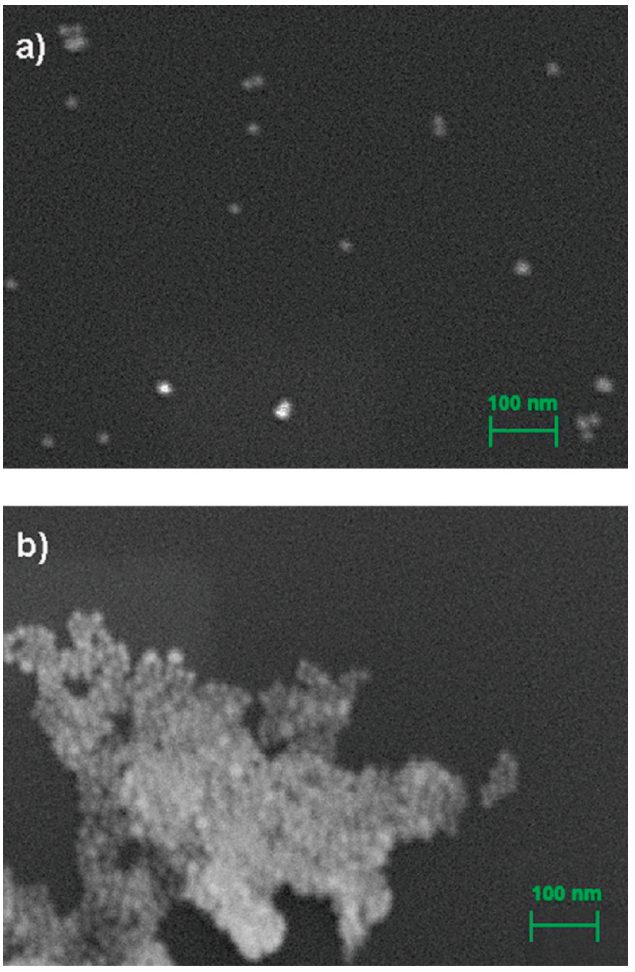

Figure 8. (a) SEM image of DNA-AuNP conjugate **Au18** employing 7-deaza-6-thio-2′-deoxyguanosine (**1**) as molecular anchor in 0.1 M NaCl, 10 mM phosphate buffer (pH 7.0); (b) SEM image of the DNA-AuNP network formed by complementary conjugates **Au18** and **Au19** in 0.1 M NaCl, 10 mM phosphate buffer (pH 7.0).

precipitate was redispersed leading to a purple solution with a UV/vis maximum of 550 nm (Figure 6b, green curve). Although the experiments was repeated several times, no network formation was observed for the complementary conjugates **Au24** and **Au25** containing 2-thio-2′-deoxythymidine (**4**), even after prolonged incubation of 1−2 weeks. The absorption maximum of the DNA-AuNP solution of **Au24** and **Au25** remained unchanged at around 524 nm (Figure 6d).

Taking together with the results summarized in Table 3, it can be concluded that, from all tested thionucleosides (**1**−**4**), the capability of 7-deaza-6-thio-2′-deoxyguanosine (**1**) as component of DNA oligonucleotides to form stable DNA gold nanoparticle conjugates is superior to that of thionucleosides **2**−**4**. DNA-AuNPs containing **1** are of comparable stability to those obtained from oligonucleotides containing the hexylthiol linker. On the contrary, thionucleosides **2**−**4** showed different drawbacks. For thionucleoside **2**, the time required for hybridization was much longer than for **1**. Up to now, we do not have an explanation regarding the prolonged incubation time required for the DNA-AuNP network formation of DNA-AuNPs with 6-thio-2′-deoxyguanosine (**2**) as molecular anchor. DNA-AuNPs with **3** and **4** were unstable in the presence of higher NaCl

dx.doi.org/10.1021/bc200069j |*Bioconjugate Chem.* 2011, 22, 794–807

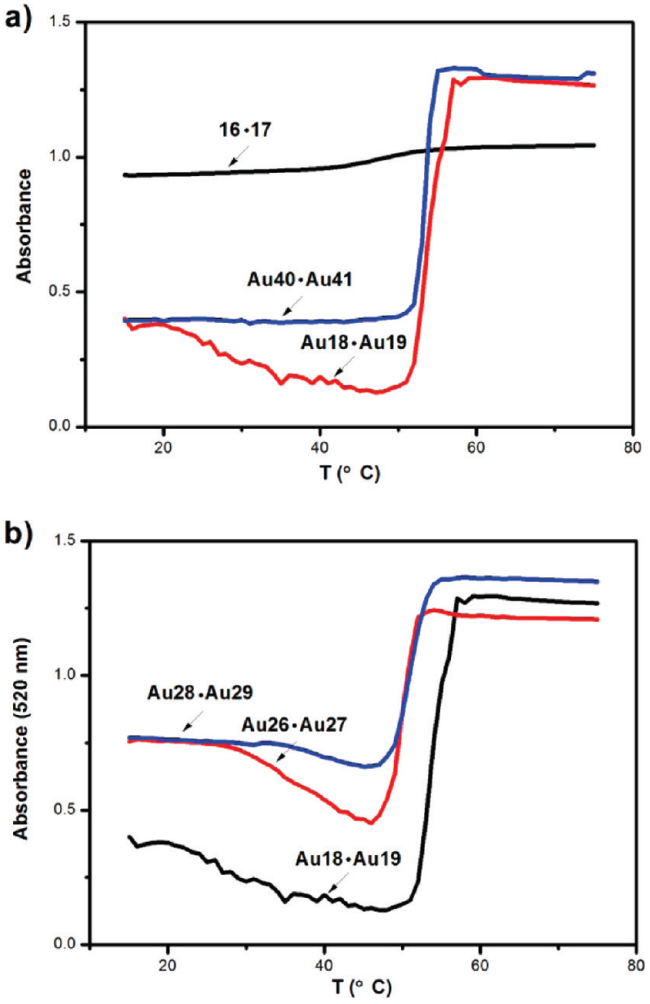

Figure 9. (a) Melting profile of the free duplex **16•17** determined at 260 nm (blue curve), and melting profiles of the DNA-AuNP assemblies of **Au18•Au19** (red curve) and **Au40•Au41** (blue curve) determined at 520 nm. (b) Melting profiles of the DNA-AuNP assemblies of **Au18•Au19** (black curve), **Au26•Au27** (red curve), and **Au28•Au29** (blue curve) determined at 520 nm.

concentration, and in addition, DNA-AuNPs with **4** are incapable of hybridization.

Thus, exemplarily, we selected DNA-AuNP solutions containing **1** to perform scanning electron microscopy (SEM) to visualize network formation. A representative section of an image showing the DNA-AuNP network formed by complementary conjugates **Au18** and **Au19** containing thionucleoside **1** is presented in Figure 8b. The SEM image shows the formation of large assembled networks of DNA-AuNP conjugates. Besides the assembled network, the neighboring area is remarkably "empty". For comparison, SEM images of nonassembled DNA-AuNP conjugates, such as **Au18** (Figure 8a), show small clusters of DNA-AuNPs which are fairly regularly distributed. The formation of large assembled networks as in Figure 8b was not observed in the case of **Au18**.

On the basis of the above-described results, melting studies were focused on DNA-AuNP conjugates employing thionucleoside **1** at different positions within the oligonucleotide chain. For comparison, T_m values were also determined for DNA-AuNP conjugates utilizing the hexylthiol linker. For this, the solutions

Table 5. T_m Values of DNA-AuNP Assemblies Incorporating Thionucleoside 1 and the Hexylthiol Linker.[a,b,c]

DNA-AuNP Assemblies	T_m [°C]
5′-d(**1** T_{10} TAG GTC AAT ACT) (**Au18**) 3′-d(ATC CAG TTA TGA T_{10} **1**) (**Au19**)	54
5′-d(**11** T_{10} TAG GTC AAT ACT) (**Au26**) 3′-d(ATC CAG TTA TGA T_{10} **11**) (**Au27**)	50
5′-d(**111** T_{10} TAG GTC AAT ACT) (**Au28**) 3′-d(ATC CAG TTA TGA T_{10} **111**) (**Au29**)	51
5′-d(TA**1** GTC AAT ACT TAG GTC AAT ACT) (**Au36**) 3′-d(ATC CAG TTA TGA ATC CAG TTA T**1**A) (**Au37**)	53
5′-d(TAG GTC AAT ACT TA**1** GTC AAT ACT) (**Au38**) 3′-d(ATC CAG TTA T**1**A ATC CAG TTA TGA) (**Au39**)	*n.m.*
5′-d(**S**-$(CH_2)_6$ T_{10} TAG GTC AAT ACT) (**Au40**) 3′-d(ATC CAG TTA TGA T_{10}-$(CH_2)_6$-**S**) (**Au41**)	53

[a] Measured at 520 nm in 0.1 M NaCl, 10 mM phosphate buffer (pH 7.0), with A_{520} = 2.1 for each DNA-AuNP conjugate solution. [b] Red ball = 15-nm-diameter gold nanoparticle. [c] Spacer T_{10} = 5′-d(TTT TTT TTT T). *n.m.* no melting observed.

containing the DNA-AuNP networks were heated (15 °C → 75 °C), and the vis absorption change at 520 nm was observed while stirring the DNA-AuNP solution. The T_m values were determined by taking the maximum of the first derivative of a melting transition and are enlisted in Table 5.

A typical sharp melting profile of **Au18•Au19** is shown in Figure 9a indicating a T_m value of 54 °C for the network of DNA-AuNPs assembled by duplex **18•19**. For comparison, the dissociation of the network formed by the conjugates **Au40** and **Au41** containing complementary oligonucleotides with hexylthiol linker was investigated under exactly the same conditions as described for the **Au18•Au19** assembly. For **Au40•Au41**, an almost identical T_m value of 53 °C was determined (Figure 9a and Table 5). It should be noted that both assemblies employ the same sequence consisting of a 12-mer oligonucleotide for base pairing and a 10-mer poly dT spacer, while the only difference is the molecular anchor being 7-deaza-6-thio-2′-deoxyguanosine (**1**) for **Au18•Au19** and the hexylthiol linker for **Au40•Au41**. Moreover, both assemblies exhibit melting profiles with a very narrow melting transition (about 4 °C) as demonstrated in Figure 9a, whereas for the parent free oligonucleotide duplex **16•17**, melting occurs over a much broader temperature range (about 20 °C) (Figure 9a). This finding is consistent with observations made earlier by others reporting that oligonucleotide duplexes covalently bound to gold nanoparticles show highly cooperative melting properties of the network forming duplexes, which is reflected by a sharp melting transition.[12,18,49]

Next, complementary DNA-AuNPs functionalized with multiple 5′-terminal thionucleosides **1** were allowed to hybridize (→ **Au26•Au27**, **Au28•Au29**). In both cases, the recognition sequence of **18•19** was used together with the 5′-d$(T)_{10}$ linker as described above. As shown in Table 5, these conjugate

assemblies exhibit very similar T_m values (**Au26•Au27**: T_m = 50 °C; **Au28•Au29**: T_m = 51 °C). The melting profiles of **Au26•Au27** and **Au28•Au29** also display a narrow melting transition range (around 4 °C) and are depicted in Figure 9b. However, compared to the T_m value found for the assembly **Au18•Au19** employing only one thionucleoside **1** per oligonucleotide strand, these values are 3−4 °C lower but still within the same range.

The melting behavior of complementary DNA-AuNP conjugates carrying 24-mer oligonucleotides which use thionucleoside **1** as anchor molecule at internal positions within their sequence was also investigated (**Au36-Au39**, Table 5). The oligonucleotides of **Au36-Au39** are composed of a twofold repeated recognition sequence allowing formation of 24 base pairs or partial hybridization (12 base pairs).

The DNA-AuNP conjugates **Au38** and **Au39** employing 24-mer complementary oligonucleotides with compound **1** located in the center of each oligonucleotide cannot form a DNA-AuNP interlinked network. Even prolonged incubation did not lead to a color change of the combined conjugate solution, and no shift of the vis maximum was observed. Thus, it can be concluded that no hybridization occurred, which is due to the negative effect of an internal thiooxo group on hybridization. Moreover, hybridization is probably additionally hindered by the short distance to the immobilization site of the gold nanoparticles.

On the contrary, a T_m value of 53 °C was detected for the closely related assembly **Au36•Au37** with thionucleoside **1** being located at the periphery of the 24-mer oligonucleotide sequences. This T_m value is consistent with that of **Au18•Au19** employing a complementary 12-mer duplex for assembly. In this regard, the observed T_m value points to a partial hybridization of the complementary oligonucleotides within the DNA-AuNP assembly. Two principle situations appear to be most conclusive, (i) a matched duplex with fraying ends and base pairing only in the center of the duplex and (ii) a shift of the complementary sequences with respect to each other leading to partial hybridization of the duplex and leaving the unpaired nucleosides as spacers between the recognition site and the gold nanoparticles. We think that a partial overlap of the recognition sites are responsible for the almost identical T_m values of **Au36•Au37** and **Au18•Au19**. Thus, the second recognition element is acting simply as spacer extending the distance to the gold nanoparticles not taking part in the hybridization process.

CONCLUSIONS

We have shown that thiooxo groups of base-modified nucleosides can be used as molecular anchors to conjugate oligonucleotides to gold nanoparticles. Compared to already existing gold nanoparticle conjugation protocols, the new linker strategy simplifies immobilization of oligonucleotides to gold nanoparticles. The method reduces additional steps such as (i) detritylation of the linker with silver nitrate which has to be performed immediately before the conjugation reaction and (ii) removal of excess silver nitrate, followed by (iii) desalting of the oligonucleotide.

Thionucleosides can be used in place of canonical DNA constituents. Incorporation of the sulfur containing nucleosides can be performed at any position of an oligonucleotide; even multiple incorporations are feasible, which will increase the binding stability of the corresponding oligonucleotides to the gold nanoparticles. 7-Deaza-6-thio-2′-deoxyguanosine (**1**) shows advantages over other thionucleosides, such as **2**−**4**, regarding stability during oligonucleotide synthesis, deprotection, and purification. Thus, solid-phase synthesis with phosphoramidites, e.g., with **6**, as well as enzymatic polymerization with corresponding triphosphates employing polymerases or terminal transferases can be performed. 7-Deaza-6-thio-2′-deoxyguanosine (**1**) can replace dG. The lower stability of nucleoside **1**•dC base pairs compared to those with dG or 7-deaza-2′-deoxyguanosine resulting from the bulkiness of the thiooxo group will not affect hybridization when the incorporation of **1** occurs outside of the recognition sequence. UV/vis spectra and hybridization properties of DNA-AuNP conjugates using thionucleoside **1** as molecular anchor reveal properties which are comparable to those containing the commercial hexanethiol linker.

ASSOCIATED CONTENT

Supporting Information. MALDI-TOF mass data of oligonucleotides, $^{1}H-^{13}C$ coupling constants, protocol of alkaline hydrolytic stability of thiooxonucleosides, HPLC profiles of the hydrolytic stability of thiooxonucleoside, UV/vis spectra of DNA-AuNP conjugates, UV/vis spectra of DNA-AuNP conjugates in high salt buffer, ^{1}H-, ^{13}C-, and ^{31}P NMR spectra of the synthesized compounds. This material is available free of charge via the Internet at http://pubs.acs.org.

AUTHOR INFORMATION

Corresponding Author

*Corresponding author. Prof. Dr. Frank Seela. Phone: +49(0)251 53406 500; Fax: +49(0)251 53406 857. E-mail: Frank.Seela@uni-osnabrueck.de. Homepage: www.seela.net.

ACKNOWLEDGMENT

We would like to thank Dr. Peter Leonard and Dr. Dieter Heindl for helpful discussions and support, and Mr. Suresh S. Pujari for critical reading of the manuscript. We also thank Dr. T. Koch from Roche Diagnostics GmbH, Penzberg, Germany, for the measurement of the MALDI spectra, Mr. Nhat Quang Tran for the oligonucleotide syntheses, and Dr. Chongwen Wang for SEM measurements. Financial support by the Roche Diagnostics GmbH and ChemBiotech, Muenster, Germany is highly appreciated.

REFERENCES

(1) Niemeyer, C. M., and Mirkin, C. A. (2004) *Nanobiotechnology*, Wiley-VCH, Weinheim.

(2) Mirkin, C. A., and Niemeyer, C. M. (2007) *Nanobiotechnology II*, Wiley-VCH, Weinheim.

(3) Niemeyer, C. M. (2001) Nanoparticles, proteins, and nucleic acids: biotechnology meets materials science. *Angew. Chem., Int. Ed. 40*, 4128–4158.

(4) Ghosh, P., Han, G., De, M., Kim, C. K., and Rotello, V. M. (2008) Gold nanoparticles in delivery applications. *Adv. Drug Delivery Rev. 60*, 1307–1315.

(5) Maxwell, D. J., Taylor, J. R., and Nie, S. (2002) Self-assembled nanoparticle probes for recognition and detection of biomolecules. *J. Am. Chem. Soc. 124*, 9606–9612.

(6) Zhao, H. Q., Lin, L., Li, J. R., Tang, J. A., Duan, M. X., and Jiang, L. (2001) DNA biosensor with high sensitivity amplified by gold nanoparticles. *J. Nanopart. Res. 3*, 321–323.

(7) Gothelf, K. V., and LaBean, T. H. (2005) DNA-programmed assembly of nanostructures. *Org. Biomol. Chem. 3*, 4023–4037.

(8) Baron, R., Willner, B., and Willner, I. (2007) Biomolecule-nanoparticle hybrids as functional units for nanobiotechnology. *Chem. Commun. (Cambridge, U. K.)* 323–332.

(9) Hutchings, G. J., Brust, M., and Schmidbaur, H. (2008) Gold-an introductory perspective. *Chem. Soc. Rev. 37*, 1759–1765.

(10) Daniel, M. C., and Astruc, D. (2004) Gold nanoparticles: assembly, supramolecular chemistry, quantum-size-related properties, and applications toward biology, catalysis, and nanotechnology. *Chem. Rev. 104*, 293–346.

(11) Seeman, N. C. (2003) DNA in a material world. *Nature 421*, 427–431.

(12) Mirkin, C. A., Letsinger, R. L., Mucic, R. C., and Storhoff, J. J. (1996) A DNA-based method for rationally assembling nanoparticles into macroscopic materials. *Nature 382*, 607–609.

(13) Storhoff, J. J., Elghanian, R., Mucic, R. C., Mirkin, C. A., and Letsinger, R. L. (1998) One-pot colorimetric differentiation of polynucleotides with single base imperfections using gold nanoparticle probes. *J. Am. Chem. Soc. 120*, 1959–1964.

(14) Alivisatos, A. P., Johnsson, K. P., Peng, X., Wilson, T. E., Loweth, C. J., Bruchez, M. P., Jr., and Schultz, P. G. (1996) Organization of 'nanocrystal molecules' using DNA. *Nature 382*, 609–611.

(15) Zhao, W., Lin, L., and Hsing, I. M. (2009) Rapid synthesis of DNA-functionalized gold nanoparticles in salt solution using mononucleotide-mediated conjugation. *Bioconjugate Chem. 20*, 1218–1222.

(16) Jadzinsky, P. D., Calero, G., Ackerson, C. J., Bushnell, D. A., and Kornberg, R. D. (2007) Structure of a thiol monolayer-protected gold nanoparticle at 1.1 Å resolution. *Science 318*, 430–433.

(17) Letsinger, R. L., Elghanian, R., Viswanadham, G., and Mirkin, C. A. (2000) Use of a steroid cyclic disulfide anchor in constructing gold nanoparticle-oligonucleotide conjugates. *Bioconjugate Chem. 11*, 289–291.

(18) Li, Z., Jin, R., Mirkin, C. A., and Letsinger, R. L. (2002) Multiple thiol-anchor capped DNA-gold nanoparticle conjugates. *Nucleic Acids Res. 30*, 1558–1562.

(19) Kumar, A., Phadtare, S., Pasricha, R., Guga, P., Ganesh, K. N., and Sastry, M. (2003) Assembling gold nanoparticles in solution using phosphorothioate DNA as structural interconnects. *Curr. Sci. 84*, 71–74.

(20) Lee, J. H., Wernette, D. P., Yigit, M. V., Liu, J., Wang, Z., and Lu, Y. (2007) Site-specific control of distances between gold nanoparticles using phosphorothioate anchors on DNA and a short bifunctional molecular fastener. *Angew. Chem. 119*, 9164–9168.

(21) Agris, P. F. (1996) The Importance of being modified: roles of modified nucleosides and Mg^{2+} in RNA structure and function, *Progress in Nucleic Acid Res and Molecular Biology* (Waldo, E. C., and Klvle, M., Eds.) pp 79−129, Vol. 53, Academic Press, New York.

(22) Rao, T. S., Durland, R. H., Seth, D. M., Myrick, M. A., Bodepudi, V., and Revankar, G. R. (1995) Incorporation of 2′-deoxy-6-thioguanosine into G-rich oligodeoxyribonucleotides inhibits G-tetrad formation and facilitates triplex formation. *Biochemistry 34*, 765–772.

(23) Nikiforov, T. T., and Connolly, B. A. (1991) The synthesis of oligodeoxynucleotides containing 4-thiothymidine residues. *Tetrahedron Lett. 32*, 3851–3854.

(24) Waters, T. R., and Connolly, B. A. (1992) Straightforward synthesis of 6-thiodeoxyguanosine and its incorporation into oligodeoxynucleotides. *Nucleosides Nucleotides Nucleic Acids 11*, 985–998.

(25) Yoshida, S., Yamada, M., Masaki, S., and Saneyoshi, M. (1979) Utilization of 2′-deoxy-6-thioguanosine 5′-triphosphate in DNA synthesis *in vitro* by DNA polymerase α from calf thymus. *Cancer Res. 39*, 3955–3958.

(26) Seela, F., Steker, H., Driller, H., and Bindig, U. (1987) 2-Amino-2′-desoxytubercidin und verwandte Pyrrolo[2,3-*d*]pyrimidinyl-2′-desoxyribofuranoside. *Liebigs Ann. Chem.* 15–19.

(27) User's manual of the DNA synthesizer, Applied Biosystems, Weiterstadt, Germany.

(28) Graham, D., Parkinson, J. A., and Brown, T. (1998) DNA duplexes stabilized by modified monomer residues: synthesis and stability. *J. Chem. Soc., Perkin Trans. 1* 1131–1138.

(29) Seela, F., and Driller, H. (1986) Palindromic oligonucleotides containing 7-deaza-2′-deoxyguanosine: solid-phase synthesis of d[(p)GG*AATTCC] octamers and recognition by the endodeoxyribonuclease *Eco*RI. *Nucleic Acids Res. 14*, 2319–2332.

(30) Turkevich, J., Stevenson, P. C., and Hillier, J. (1951) A study of the nucleation and growth processes in the synthesis of colloidal gold. *Discuss. Faraday Soc. 11*, 55–57.

(31) Demers, L. M., Mirkin, C. A., Mucic, R. C., Reynolds, R. A., Letsinger, R. L., Elghanian, R., and Viswanadham, G. (2000) A fluorescence-based method for determining the surface coverage and hybridization efficiency of thiol-capped oligonucleotides bound to gold thin films and nanoparticles. *Anal. Chem. 72*, 5535–5541.

(32) Seela, F., Budow, S., and Leonard, P. (2007) Oligonucleotides forming an i-motif: the pH-dependent assembly of individual strands and branched structures containing 2′-deoxy-5-propynylcytidine. *Org. Biomol. Chem. 5*, 1858–1872.

(33) Seela, F., and Budow, S. (2006) pH-Dependent assembly of DNA-gold nanoparticles based on the i-motif: a switchable device with the potential of a nanomachine. *Helv. Chim. Acta 89*, 1978–1985.

(34) Beermann, B., Carrillo-Nava, E., Scheffer, A., Buscher, W., Jawalekar, A. M., Seela, F., and Hinz, H.-J. (2007) Association temperature governs structure and apparent thermodynamics of DNA-gold nanoparticles. *Biophys. Chem. 126*, 124–131.

(35) Dinu, C. Z., Opitz, J., Pompe, W., Howard, J., Mertig, M., and Diez, S. (2006) Parallel manipulation of bifunctional DNA molecules on structured surfaces using kinesin-driven microtubules. *Small 2*, 1090–1098.

(36) Erler, C., and Mertig, M. (2009) Incorporation of DNA networks into microelectrode structures. *J. Vac. Sci. Technol. B 27*, 939–943.

(37) Schulhof, J. C., Molko, D., and Teoule, R. (1987) The final deprotection step in oligonucleotide synthesis is reduced to a mild and rapid ammonia treatment by using labile base-protecting groups. *Nucleic Acids Res. 15*, 397–416.

(38) Christopherson, M. S., and Broom, A. D. (1991) Synthesis of oligonucleotides containing 2′-deoxy-6-thioguanosine at a predetermined site. *Nucleic Acids Res. 19*, 5719–5724.

(39) Newmark, R. A., and Hill, J. R. (1976) Assignment of primary and secondary amide carbonyl resonances in carbon-13 NMR. *J. Magn. Reson. 21*, 1–7.

(40) Pfeffer, P. E., Valentine, K. M., and Parrish, F. W. (1979) Deuterium-induced differential isotope shift ^{13}C NMR. 1. Resonance reassignments of mono- and disaccharides. *J. Am. Chem. Soc. 101*, 1265–1274.

(41) Winkeler, H. D., and Seela, F. (1983) Synthesis of 2-amino-7-(2′-deoxy-β-D-erythro- pentofuranosyl)-3,7-dihydro-4*H*-pyrrolo[2,3-*d*]pyrimidin-4-one, a new isostere of 2′-deoxyguanosine. *J. Org. Chem. 48*, 3119–3122.

(42) Connolly, B. A., and Newman, P. C. (1989) Synthesis and properties of oligonucleotides containing 4-thiothymidine, 5-methyl-2-pyrimidinone-1-β-D-(2′-deoxyriboside) and 2-thiothymidine. *Nucleic Acids Res. 17*, 4957–4974.

(43) Coleman, R. S., and Kesicki, E. A. (1994) Synthesis and postsynthetic modification of oligodeoxynucleotides containing 4-thio-2′-deoxyuridine ($d^{s4}U$). *J. Am. Chem. Soc. 116*, 11636–11642.

(44) Coleman, R., S., McCary, J. L., and Perez, R., J. (1999) Thionucleoside disulfides as covalent constraints of DNA conformation. *Tetrahedron 55*, 12009–12022.

(45) Milton, J., Connolly, B. A., Nikiforov, T. T., and Cosstick, R. (1993) Site-specific disulfide bridges in oligodeoxyribonucleotide duplexes containing 6-mercaptopurine and 4-thiothymine bases. *J. Chem. Soc., Chem. Commun.* 779–780.

(46) Uznanski, P., Kurjata, J., and Bryszewska, E. (2009) Modification of gold nanoparticle surfaces with pyrenedisulfide in ligand-protected exchange reactions. *Mater. Sci.-Pol. 27*, 659–670.

(47) Hurst, S. J., Lytton-Jean, A. K. R., and Mirkin, C. A. (2006) Maximizing DNA loading on a range of gold nanoparticle sizes. *Anal. Chem. 78*, 8313–8318.

(48) Marathias, V. M., Sawicki, M. J., and Bolton, P. H. (1999) 6-Thioguanine alters the structure and stability of duplex DNA and inhibits quadruplex DNA formation. *Nucleic Acids Res. 27*, 2860–2867.

(49) Jin, R., Wu, G., Li, Z., Mirkin, C. A., and Schatz, G. C. (2003) What controls the melting properties of DNA-linked gold nanoparticle assemblies? *J. Am. Chem. Soc. 125*, 1643–1654.